Songklanakarin J. Sci. Technol.
45 (3), 363–370, May – Jun. 2023

http://www.sjst.psu.ac.th

Original Article

Evidence of coastal landforms and age determination related to the sea-level change at Nakhon Si Thammarat province in southern Thailand

Parisa Nimnate[1, 2*], Santi Pailoplee[2], Montri Choowong[2], and Sasinaree Visedpadsa[1]

[1] *Division of Geoscience, Mahidol University, Kanchanaburi Campus, Sai Yok, Kanchanaburi, 71150 Thailand*

[2] *Center of Excellence for the Morphology of Earth Surface and Advanced Geohazards in Southeast Asia (MESA CE), Department of Geology, Faculty of Science, Chulalongkorn University, Pathum Wan, Bangkok, 10330 Thailand*

Received: 12 January 2023; Revised: 19 March 2023; Accepted: 6 April 2023

Abstract

We present evidence of sea-level changes over the past 15,000 years from dating sandy beach sediments in Nakhon Si Thammarat province. First, we classified various types of coastal landforms from satellite images. The orientations of beach ridges and old lagoons are very important to understanding the evolution of sea-level rise and fall. In this area, there were two groups of old sandy beaches: (i) the inner beach, and (ii) the outer beach, which were separated by old lagoons. Then, nine quartz-rich samples were analyzed using Optically Stimulated Luminescence analysis to estimate the ages of deposition. The results supported the concept that the inner series of old sandy beach deposits indicated the onset of sea-level regression occurring approximately 15,000 years ago (YA). Sea level still stands, derived from the erosion of the beach ridge and deposition of old tidal flats, were estimated to be between 10,000 and 4,000 YA. The old lagoon showed a period of being covered from approximately 4,000 to 2,000 YA before outer beach ridge deposition some 2,000 to 400 YA during sea-level regression. Considering these measured ages, the sandy beach sediments yield the oldest range of depositional ages among all the Holocene beach deposits in southern Thailand.

Keywords: old sandy beach, OSL dating, sea-level change, Nakhon Si Thammarat, Thailand

1. Introduction

Coastal areas are dynamic and their evolution is related to climate change and sea level history, especially in the coastal plain along the Gulf of Thailand. To better understand the geological record of marine transgression and regression, a combination of ancient geomorphological landforms and radiometric dating (i.e., radiocarbon dating) have become crucial sources of information for determining the history of sea level changes (Choowong *et al.*, 2004, 2011; Sinsakul, 1992; Williams *et al.*, 2016). However, Optically Stimulated Luminescence (OSL) analysis is also a robust dating tool to explore the evolution of Quaternary marine coastal facies and landforms (Lamothe, 2016). Precise altitudes of each beach ridge coupled with reliable results of dating can reveal the migration rate of beach-ridge progradation as well as proxies of sea-level change (Karpytchev, 1993) that are directly related to the deposition of sediment in the environment at that time.

Conceptually, OSL dating is capable of dating quartz-rich sediments that have been exposed to daylight up to the date of their last deposition, for periods ranging from months to 150,000 years (Murray & Olley, 2002; Murray & Wintel, 2000). As a result, several studies of coastal sandy sediments using OSL dating have reported the effectiveness of this technique, i.e., the OSL dating of beach dune sequence in Australia (Banerjee *et al.*, 2003), marine terrace sediments in Korea (Choi, Murray, Jain, Cheong, & Chang, 2003), beach

*Corresponding author
Email address: parisa.nim@mahidol.edu

ridge plain in Denmark (Nielsen, Murray, Pejrup, & Elberling, 2006), paleo shorelines in Tibet (Lee, Li, & Aitchison, 2009), coastal barrier spit in Germany (Reimann, Naumann, Tsukamoto, & Frechen, 2010), and the study of coastal dune and beach ridge deposits in Thailand (Miocic *et al.*, 2022; Nimnate, Chutakositkanona, Choowong, Pailoplee, & Phantuwongraj, 2015; Surakiatchai *et al.*, 2019). Moreover, the evidence of sand deposition between offshore bar and beach berm indicates the effect by aeolian process during the sea-level highstand in the last interglacial in Songkhla (Noppradit, 2019). To establish the evolution of the coast in southern Thailand, old sandy beach sediments along Nakhon Si Thammarat Province (NSTP) were investigated and analyzed chronologically for their depositional ages. The ages obtained will be useful in estimating the regional evolution of the sea-level change in the period of beach ridge development.

2. Materials and Methods

2.1 Study area and sampling location

In southern Thailand the locations of prior research related to sea-level changes in the past are shown as black dots in Figure 1a (Nimnate *et al.*, 2015; Polwichai, 2017; Sainakum *et al.*, 2021; Surakiatchai *et al.*, 2018). Based on detailed remote sensing interpretation (Figure 1b, c) from digital elevation data, a geomorphic map of this area was created to plan the sampling locations (Figure 1d, e) for obtaining evidence of sea-level changes, possibly preserved as beach ridges (blue color in Figure 1c). From the derived geomorphic map, at least seven units of different geomorphologic landforms were classified, including mountain, beach (recent), old sandy beach (defined as a paleo sand spit in this study), old alluvium (white square in Figure 1b), tidal flat, old tidal flat, and old lagoon (Figure 1c). Among these interpreted landforms, the old sandy beach at NSTP is composed of two series, i.e., the inner and the outer beach ridge series (Figure 1c). The inner ridge in the northern and central parts of the study area forms a single ridge apart from some parts that were blanketed by colluvium deposit (see the white square in Figure 1b). In the northern part, inner and outer beach ridges were located about 4 and 6 km landwards from the present-day shoreline (Figure 1d). Meanwhile, in the southern part the beach ridges were located about 40 and 25 km inland, respectively (Figure 1d). The southern part of the inner beach ridge spat to nine ridges that are generally slightly lying in a northwest-southeast direction and concave towards the sea (Figure 1e). The outer beach ridge in the northern and southern parts of NSTP spat to a small beach ridge. The old lagoon separated the inner and outer ridges (pink color in Figure 1c). To clarify the ages of beach deposition, a total of four samples (NK1–4) were collected for the inner beach ridges and five samples (NK5–9) from the outer beach ridge (Figure 1c, d).

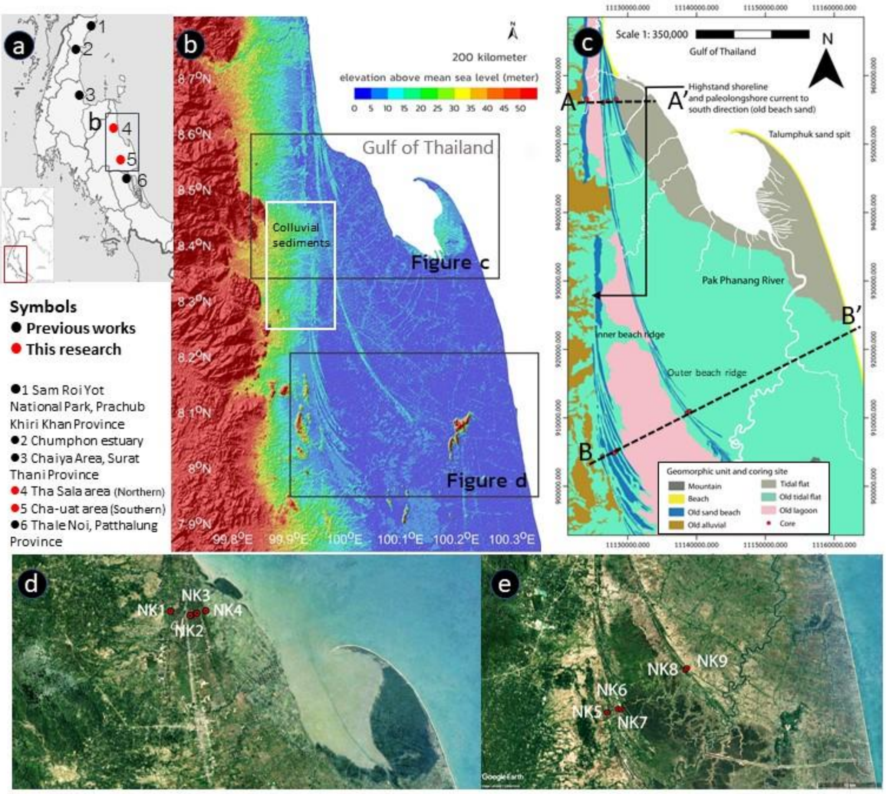

Figure 1. Geographical location of Nakhon Si Thammarat province and adjacent area in southern Thailand. (a) Southern Thailand map and locations of related previous work (shown in black dots: 1. Surakiatchai *et al.*, 2018; 2. Nimnate *et al.*, 2015; 3. Polwichai, 2017; and 6. Sainakum*et al.*, 2021 and this work (red dots). (b) Terrain map of the NSTP showing the locations of the inner and outer old sandy beaches. (c) Geomorphological map interpreted from the terrain map. (d) Location of the OSL sampling in the northern part: line A-A' (NK1–4) (e) Location of the OSL sampling in the southern part: line B-B' (NK5–9)

2.2 Dating by OSL analysis

Conceptually, the period between the last deposition of sediment (beaching to sunlight) and the present can be determined by OSL dating using Equation (1) (Aitken, 1985);

$$\text{OSL date} = \frac{\text{Equivalent dose (ED)}}{\text{Annual dose (AD)}} , \qquad (1)$$

where the equivalent dose (ED; unit of Gy) was measured from the luminescence emitted during the OSL analysis of the sample. Meanwhile, the dose rate or annual dose (AD; unit of Gy/Ka) was evaluated from the concentration of three abundant natural radioisotopes [uranium (U), thorium (Th), and potassium (K)] and the water content, in the environment surrounding the sample.

In the sample collection process, each sample (NK1–9 in Figure 1c, d) was divided into two portions and used for evaluating the (i) ED and (ii) AD including the water content. Regarding the ED sampling, the unit of topsoil was eliminated, and the pit was dug until the quartz-rich sediment, representing the beach ridge, was exposed (a depth of around 30–50 cm). After preparing the subdue environment, the surface of the sediment profile was eliminated to avoid present-day exposure to the sunlight. Thereafter, the quartz-rich sediment was collected to conform to the lamination and bedding. To avoid leakage of the ED signal, the samples were taken in plastic tubes, sealed immediately to retain moisture, and stored in lightproof plastic bags. Thereafter, some parts of sand were additionally collected at a 30-cm depth surrounding the ED sampling location and used for the AD evaluation.

2.3 Evaluation of the ED

In an individual ED sample of NK1–9, the sample was enriched for quartz by extraction following the reported procedure (Surakiatchai *et al.*, 2018; Takashima & Honda, 1989). First, a wet sieve (mesh no. 60–200) was employed to recover fine to very fine grain sands of 74–250 μm diameter. Second, the sample was etched with hydrochloric acid to eliminate the carbonate portion. Third, the sample was treated with hydrofluoric acid to remove any feldspar contamination in sample. Thereafter, the sample was washed with distilled water and then dried at 100 °C. Finally, the ferro minerals were eliminated using an iso-dynamic magnetic separator.

The ED measurements were performed using a Risø TL/OSL reader at the Department of Geology, Faculty of Science, Chulalongkorn University, Thailand. Each measurement was equipped with a calibrated 90Sr/90Y beta radiation source and a blue (400–525 nm) light source (BØtter-Jensen, 1997; BØtter-Jensen, 2000). For this OSL measurement, a detection filter of 7.5 mm (Hoya U340) was used and the sample was preheated to 220 °C at 5 °C/s. Prepared quartz grains were attached to a 9.8 mm diameter stainless-steel disc using silicone oil. A single aliquot regenerative technique was employed to assess all ED (Murray & Wintle, 2000; Readhead, 1987). A fixed test dose of 10% of the natural dose was applied to correct any sensitivity changes. The obtained OSL decay curve of the NK4 sample is demonstrated in Figure 2a, and based on this known artificial irradiation, the OSL growth curve of each aliquot was derived (Figure central age model Aliquot Regenerative (SAR) procedures. This provides more precise ages as they make it possible to obtain by interpolation a similar number of equivalent dose measurements to aliquot measurements. The main procedure revolutionized optical dating. It was recently developed for quartz grains and applied also to feldspars. The SAR procedure is now a standard protocol used in luminescence dating (Cordier, 2010). To constrain the ED, 24 discs of aliquots per sample were measured with the test dose range results ranging from 0.9–1.1 (10% sensitivity test). Conceptually, four different age models could be applied in the analysis of ED datasets, namely: (i) central or average age model, (ii) common age model, (iii) minimum age model, and (iv) finite mixture model (Takashima & Honda, 1989). The ED distribution and statistic parameters from nine samples are shown in Figure 3. The overdispersion (OD) in each case was determined and used to select the appropriate model (Liang, 2019; Duller ,2008). The OD value of the minimum age and average age models were > 25 and < 25, respectively. The obtained OSL ages used in this work are shown in bold font in Table 1 in the Age min and Avg age (year) columns (depending on the OD value (Figure3 ED distribution) the result of age determination in each location in the model (Figure 4).

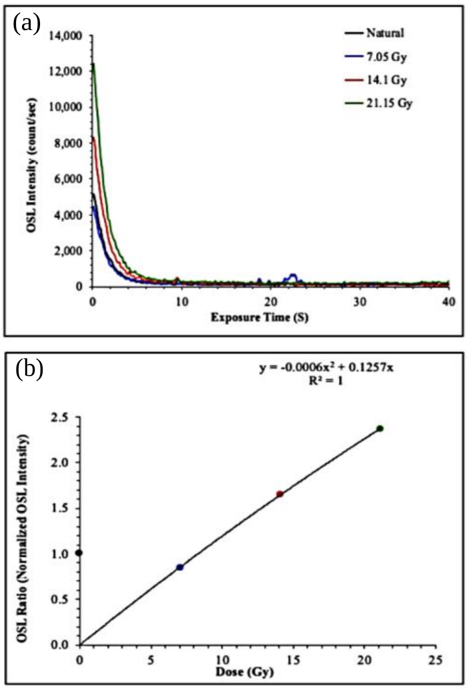

Figure 2. Representative OSL (a) decay curves and (b) growth curve of old sandy beach sample NK4, where N represents the natural (Natural = 6.78 Gy) (black dot) and single (blue dot), double (red dot), and triple regenerative doses (green dot), respectively.

2.4 Evaluation of the AD

In the context of Equation (1), a 300-g portion of the obtained grains (diameter < 90 mm) was dried and then packed in a plastic vessel ready for the AD evaluation.

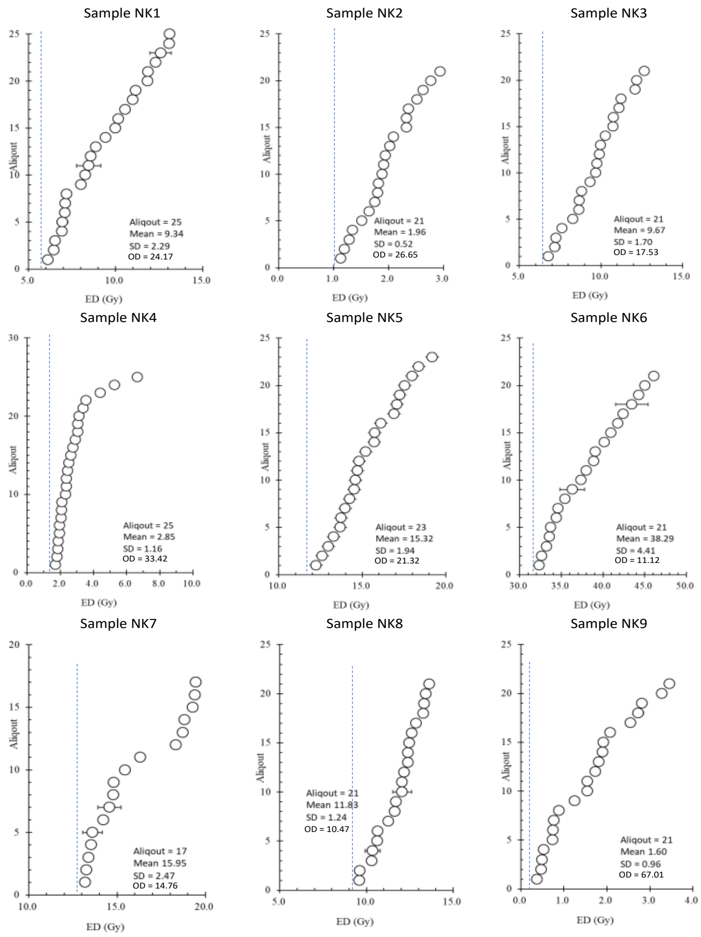

Figure 3. Graph showing the ED distributions (white circles) of the nine old sandy beach samples, Blue dashed lines define the minimum age of the samples.

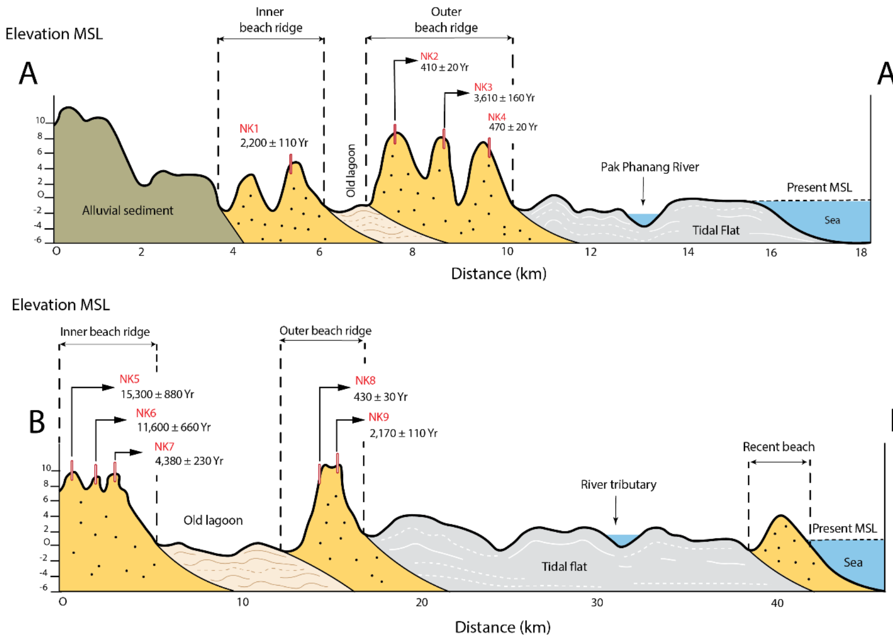

Figure 4. Cross-sections with irregular topography of the outer beach ridge, inner beach ridge, and present shoreline. The OSL dating of the paleo sandy beach sediments gave a maximum age of deposition 12,900 and 2,310 YA in the inner and outer beach ridge, respectively.

Table 1. The OSL-derived ages of the beach ridge plain at the NST. Bold fonts in ages are the ages derived from the minimum age model (Age min) and the average age model (Age avg) from the OD value (Figure 3).

Samples	Latitude (°N)	Longtitude (°E)	Dists (km)	Depth (cm)	U (ppm)	Th (ppm)	K (%)	Moist. (%)	Dose rate (Gy/Ka)	De min (Gy/)	De avg (Gy)	Age min (year)	Age min (year)
NK1	8.55	99.93	10	30	2.59±0.01	9.93±0.08	1.56±0.01	6.90	4.23±0.22	6.12±0.03	9.34	1,440±70	**2,200±110**
NK2	8.55	99.95	8	40	1.18±0.01	2.28±0.04	1.68±0.01	4.90	2.75±0.14	1.13±0.01	1.96	**410±20**	710±30
NK3	8.55	99.96	7	50	1.16±0.01	2.74±0.04	2.02±0.01	4.40	3.06±0.16	6.78±0.03	9.67	2,210±110	**3,160±160**
NK4	8.55	99.97	6	40	1.08±0.01	3.22±0.05	3.02±0.01	14.10	3.63±0.20	1.719±0.00	2.85	**470±20**	780±40
NK5	8.09	99.95	38	40	1.03±0.01	1.89±0.05	0.05±0.00	5.00	1.00±0.06	12.22±0.06	15.32	12,200±700	**15,300±880**
NK6	8.09	99.96	37	40	2.79±0.01	10.76±0.01	0.41±0.00	9.20	3.30±0.19	32.33±0.22	38.29	9,800±560	**11,600±660**
NK7	8.09	99.97	37	40	2.20±0.01	8.63±0.09	0.87±0.00	4.00	3.34±0.18	13.18±0.07	1.60	3,940±200	**4,380±230**
NK8	8.14	100.06	25	40	1.88±0.01	6.13±0.07	1.06±0.01	13.70	2.70±0.14	3.38±0.00	11.83	140±00	**430±30**
NK9	8.14	100.06	25	40	1.14±0.01	4.6±0.06	3.09±0.01	20.60	4.41±0.23	9.59±0.05	15.95	**2,170±110**	3,610±180

Dists: distance to the shore. De: total absorbed radiation dose.

The water content, as the absorbing part of the radiation, was ascertained during this process. In the measurement, the concentrations of U (ppm), Th (ppm), and K (%) were determined by high-resolution gamma spectrometry (Table 1). Based on the obtained concentration of these three radionuclides and the water content, the AD for each sample was evaluated according to the standard table, including the calculated cosmic ray dose rate (Bell, 1979; Prescott & Hutton, 1994). Thereafter, the obtained AD was reduced by attenuation factors based on both the grain size distribution and water content (Aitken, 1985). The AD of each sample and the error estimate were calculated as previously reported (Singh, Pattanaik, Gagan, & Jaiswal, 2017) and are summarized in Table 1.

Based on the obtained ED and AD of each sample, the OSL dates representing the last deposition of the sandy beach (NK1–9 in Figure 1d, e) were clarified and are shown in Table 1.

3. Results and Discussion

3.1 Radioactive elements

All of the AD measurements of beach ridge samples and the radionuclide concentrations, in the units of % K, were divided into two groups. The AD varied from 2.70 ± 0.14 Gy/Ka (NK9) to 1.00 ± 0.06 Gy/Ka (NK5), while the K ranged from 0.05 (NK5) to 3.09 ± 0.01 (NK9). Comparing the AD and %K in all samples, the %K in the samples collected in the southern part of the inner ridge series (NK5-7) was less than in all of the other samples due to the older deposition age. The lowest concentrations of U (0.05 ± 0.00 ppm) were found in NK5, which was related to this site having the oldest aged beach ridges in this area. The older sandy sediment deposit should have a low concentration of K due to leaching during weathering. K-bearing mineral is usually weathered by hydrolysis, especially in SE Asia that has had strong weathering during the last interglacial period (Verstappen, 1980; Wilford, 2012). However, the northern part of the inner beach ridge series showed a higher radionuclide concentration in K than the southern part, because these sediments were disturbed by young alluvial sediments. The outer beach ridge series also gave high K values for all the samples, and especially for samples NK4 and NK9 (3.02 ± 0.01 and 3.09 ± 0.01 ppm, respectively) due to the higher clay mineral content from the paleo tidal flat depositional environment that was deposited between the beach ridge sediment samples (Table 1).

3.2 The ages of the sandy beach deposits

Based on the OSL dates (Table 1), three inner series of beach ridges (samples NK5–7) indicated that predominantly sandy sediments were deposited at 15,300 ± 880 (for sample NK5) to 4,380 ± 230 (NK7) years ago (YA) (Figure 4b). The maximum age of the southern part of this inner series of beach ridges was 16,100 years at 10 m above the present mean sea level (AMSL) from the location where the sample NK5 was collected inland, 38 km perpendicular to the present shoreline. After deposition during regression period the sediment on the upper surface may be eroded, so the younger sediment gets transported away and the age result may represent the older sediment at the deeper layer from previous surface (Evans, 2013). The innermost inner beach ridge also indicated the sea-level highstand during the transgression period (shown by the black arrow in Figure 1c) and could indicate that the paleo-longshore current moved to a southward direction. The northern part of the inner beach ridge at the northern transect is younger than the southern part, since the deposition of alluvial sediments on top of the beach ridges started from around 2,200 ± 110 YA (Figure 4a), as revealed from the analysis of the NK1 sample (Table 1). Subsequently, the old lagoon or tidal sediment deposits occurred between the inner and outer series at that time, where the sea level still stands were at a constant level for 2,000 years, as indicated by the light brown color in Figure 3 and pink color in Figure 1c. This age conforms to the ^{14}C dating results of the fossils from the former tidal flat in the Sam Roi Yot area (no.1 in Figure 1 a) at 4,000–2,500 YA (Surakiatchai *et al.*, 2006, 2018).

The onset of sea level regression was evidenced by the presence of outer series of beach ridges with ages ranging from 3,610 ± 160 YA (NK3) to 470 ± 20 years (NK2), as shown in Table 1 and Figure 4a. The maximum age of the outer ridge was 3,610 ± 160 YA (8 m AMSL) for sample NK3 located at 7 km perpendicular distance to the present shoreline. The estimated age of NK3 is older than NK2 and NK9 is older than NK8. These may be caused by incomplete bleaching during transportation of high energy in the conditions with strong wave action, when the sediments deposit and get buried suddenly. The OSL signal then led to an overestimate of the equivalent dose, and consequently of the age (Duller, 2008; Cordier, 2010). The younger age (NK2, NK4 and NK8) may represent redeposits by aeolian process (Noppradit, 2019). This result conforms to the OSL age (110–2,000 YA) (Polwichai, 2017) from Leam Pho in Chaiya district, Surat Thani province (located as black dot no. 3 in Figure 1a). At the end point of the outer beach ridge, where sample NK4 was collected, this sand ridge was separated into two smaller ridges engulfed by old tidal flat sediments and the present sandy beach sediments to the east.

3.3 Sea-level evolution in southern Thailand

The inner and outer paleo beach ridges at the NSTP depicted a series of discontinuous slightly-curved ridges in the southern part separated by an old lagoon from the late Pleistocene to the late Holocene. On the other hand, the west coast of the gulf mostly preserved the record of the middle Holocene high stand at Chumphon estuary (black dot no.2 in Figure 1a) and Thai-Malay peninsula, where the age of the high stand was reported previously to be about 6,500 YA with a high stand of about 4 m AMSL (Horton *et al*., 2005; Nimnate *et al*., 2015). Only the maximum age of the beach ridge at NSTP provided the time of marine transgression of this research at around 16,00**0** YA at about 8 m AMSL, which suggested the age of the high stand. The deposition comparatively corresponded with the age of the late Pleistocene to Early Holocene marine transgression (Choowong, 2011).

These inner beach ridges formed during 15,300 ± 880 to 11,600 ± 660 YA at about 9–10 m AMSL (NK5 and NK6) and were related to the meltwater pulse (MWP)-1B that led to an average sea-level rise of 15 m between 11,500 and 11,200 years YA (Fairbanks, 1989). After that, during the MWP-1C with a 6.5 m sea-level rise during 9,500–9,200 YA (Blanchon & Shaw, 1995; Liu & Milliman, 2004; Törnqvist, 2004), the inner beach ridges had a very low depositional rate or the inner ridge sediments got eroded due to being flooded by the transgression at 8,500 years BP, based on the radiocarbon analysis from Thale Noi at Patthalung province (black dot no. 6 in Figure 1a) (Chabangborn *et al.*, 2020; Chaimanee, 1986). The rapid sea-level rise at 8,500 YA has also been recognized from the geochemical records from Singapore (Bird *et al.*, 2010). The results from the n-alkanes analysis are also in accord with a sea-level rise around 7,500-7,300 YA in Patthalung province (black dot no.6 in Figure 1a) (Sainakum, Jittangprasert, Sompongchaiyakul, & Jirapinyakul, 2021). The outermost inner sandy ridge deposit has a maximum age of 4,600 YA (NK7).

In the study area, the old lagoon sediment was deposited from 4,000 to 2,000 YA, which indicates a sea level stand still at that time. The outer beach ridge gave a maximum age of 3,610 years at about 8 m AMSL, which suggested the age of the transgression. Similarly, the outer beach ridge at Chumphon province (black dot no.2 in Figure 1a) provided an age of 3,800–1,600 YA (Nimnate *et al*., 2015). The absence of beach ridges is because during that time the open sea environment provided inappropriate accommodation space for preserving rapid beach ridge transgression (Surakiatchai *et al.*, 2019). Moreover, the tidal flat deposited before changing the depositional environment to the recent sandy beach.

4. Conclusions

This study presents the first OSL dating application of young Holocene sediments from the coastal environment in NSTP. Nine samples were taken in Tha Sala to Cha-Uat Districts (red dots no. 4 and 5 in Figure 1a) from beach ridges to reconstruct the development of the beach ridge sand and spit system. The SAR protocol was applied to coarse grained quartz for OSL dating. Overall, the results from the OSL age of two series of inner beach ridges suggest that sea-level transgression first started around 15,000 YA and the beginning of regression with deposition of the inner beach ridge series to the east direction coincided with the alignment of the beach ridge. After that, the sea level remained at the same level forming the lagoon environment, where the beach sand was changed to a marsh and lagoon environment that was deposited during the sea-level stand still, i.e., seawater flooded this area. The deposition at this time, during 4,300–2,300 YA in the southern and northern area, depended on the sediment type and properties. The deposited outer beach ridge sediments were formed at 3,700 to 440 YA and revealed an obvious occurrence of the outer beach ridge deposition, and then the environment changed to a tidal flat from 400 YA due to sea-level regression to the present location and forming the recent beach.

Acknowledgements

All sampling was performed during 2019 by Sasinaree Visedpadsa with assistance from Nattapon Nakapa, Ittipong Anupan and Panupong Srisuwan. The Laboratory for Luminescence Dating provided advice on sampling and data analysis, as well as performed the measurements of most samples, involving Sutthikan Khamsiri and laboratory staff from the Department of Geology, Chulalongkorn University, and Panas Hong from Mahidol University Kanchanaburi Campus. Constructive comments on the manuscript were received from Assist. Professor Dr. Akkaneewut Jirapinyakul.

References

Aitken, M. J. (1985). *Thermoluminescence dating*. London, England: Academic Press.

Banerjee, D., Hildebrand, A. N., Murray-Wallace, C. V., Bourman, R. P., Brooke, B. P., & Blair, M. (2003). New quartz SAR-OSL ages from the stranded beach dune sequence in south-east South Australia. *Quaternary Science Reviews*, *22*(10), 1019-1025. doi:10.1016/S0277-3791(03)00013-1

Bell, W. T. (1979). Attenuation factors for the absorbed radiation dose in quartz inclusions for Thermo-luminescence dating, *Ancient TL, 8*, 2-13. doi: 10.1016/1359-0189(87)90037-9

Bird, M. I., Austin, W. E., Wurster, C. M., Fifield, L. K., Mojtahid, M., & Sargeant, C. (2010). Punctuated eustatic sea-level rise in the early mid-Holocene. *Geology*, *38*(9), 803-806. doi:10.1130/G31066.1

Blanchon, P., & Shaw, J. (1995). Reef drowning during the last deglaciation: Evidence for catastrophic sea-level rise and ice-sheet collapse. *Geology*, *23*, 4-8. doi:10.1130/0091-7613(1995)023<0004:RDDTLD>2.3.CO;2

BØtter-Jensen, L. (1997). Luminescence techniques: Instrumentation and methods. *Radiation Measurements*, *27*(5), 749-768. doi:10.1016/S1350-4487(97)00206-0

Bøtter-Jensen, L., Bulur, E., Duller, G. A. T., & Murray, A. S. (2000). Advances in luminescence instrument systems. *Radiation Measurements*, *32*(5), 523-528. doi:10.1016/S1350-4487(00)00039-1

Chabangborn, A., Punwong, P., Phountong, K., Nudnara, W., Yoojam, N., Sainakum, A., & Sompongchaiyakul, P. (2020). Environmental changes on the west coast of the Gulf of Thailand during the 8.2 ka event. *Quaternary International*, *536*, 103-113. doi:10.1016/j.quaint.2019.12.020

Chaimanee, N., Teeyapan, S., Teerarungsigul, N. (1986). Geology of Amphoe Cha-Uat and Amphoe Ranot.

Choi, J. H., Murray, A. S., Jain, M., Cheong, C. S., & Chang, H. W. (2003). Luminescence dating of well-sorted marine terrace sediments on the southeastern coast of Korea. *Quaternary Science Reviews*, *22*(2), 407-421. doi: 10.1016/S0277-3791(02)00136-1

Choowong, M. (2011). *Book series on geology of Thailand*. London, England: Geological Society of London

Choowong, M., Ugai, H., Charoentitirat, T., Charusiri, P., Daorerk, V., Songmuang, R., & Ladachart, R. (2004). Holocene Biostratigraphical records in coastal deposits from Sam Roi Yod National Park, Prachuap Khiri Khan, Western Thailand. *Tropical Natural History*, *4*(2), 1-18.

Cordier, S. (2010). Optically stimulated luminescence dating: Procedures and applications to geomorphological research in France. *Géomorphologie*, *16*(1), 21–40. doi:10.4000/geomorphologie.7785

Duller, G. A. T. (2008). Single-grain optical dating of Quaternary sediments: Why aliquot size matters in luminescence dating. *Boreas*, *37*(4), 589-612. doi:10.1111/j.1502-3885.2008.00051.x

Evans, D. J. A. (2013). Glacial landforms, sediments | Glacial sequence stratigraphy. In S. A. Elias & C. J. Mock (Eds.), *Encyclopedia of Quaternary Science* (2nd ed., pp. 85-90). Amsterdam, The Netherlands: Elsevier.

Fairbanks, R. G. (1989). A 17,000-year glacio-eustatic sea level record: influence of glacial melting rates on the Younger Dryas event and deep-ocean circulation. *Nature*, 342(6250), 637-642. doi:10.1038/342637a0

Horton, B., Gibbard, P., Milne, G. M., Morley, R., Ltd, P., & Purintavaragul, C. (2005). Holocene sea levels and palaeoenvironments, Malay-Thai Peninsula, Southeast Asia. *Holocene*, 15. doi:10.1191/0959683605h891rp

Karpytchev, Y. A. (1993). Reconstruction of Caspian Sea level fluctuations: Radiocarbon dating coastal and bottom deposits. *Radiocarbon*, 35, 409-420. doi:10.1017/S0033822200051742

Lamothe, M. (2016). Luminescence dating of interglacial coastal depositional systems: Recent developments and future avenues of research. *Quaternary Science Reviews*, 146, 1-27. doi: 10.1016/j.quascirev.2016.05.005

Lee, J., Li, S., & Aitchison, J. (2009). OSL dating of paleoshorelines at Lagkor Tso, western Tibet. *Quaternary Geochronology*, 4, 335-343. doi:10.1016/j.quageo.2009.02.003

Liang, P. (2019). LDAC: An Excel-based program for luminescence equivalent dose and burial age calculations. *Ancient TL*, 37, 21-40.

Miocic, J., Sah, R., Chawchai, S., Surakiatchai, P., Choowong, M., & Preusser, F. (2022). High resolution luminescence chronology of coastal dune deposits near Chumphon, Western Gulf of Thailand. *Aeolian Research*, 56, 100797. doi:10.1016/j.aeolia.2022.100797

Murray, A., & Olley, J. (2002). Precision and accuracy in the optically stimulated luminescence dating of sedimentary quartz: A status review. *Geochro nometria*, 21.

Murray, A. S., & Wintle, A. G. (2000). Luminescence dating of quartz using an improved single-aliquot regenerative-dose protocol. *Radiation Measure ments*, 32(1), 57-73. doi:10.1016/S1350-4487(99)00253-X

Nielsen, A., Murray, A. S., Pejrup, M., & Elberling, B. (2006). Optically stimulated luminescence dating of a Holocene beach ridge plain in Northern Jutland, Denmark. *Quaternary Geochronology*, 1(4), 305-312. doi:https://doi.org/10.1016/j.quageo.2006.03.001

Nimnate, P., Chutakositkanona, V., Choowong, M., Pailoplee, S., & Phantuwongraja, S. (2015). Evidence of Holocene sea level regression from Chumphon coast of the Gulf of Thailand. *ScienceAsia*, 41(1), 55-63. doi:10.2306/scienceasia1513-1874.2015.41.055

Noppradit, P., Schmidt, C., Dürrast, H., & Zöller, L. (2019). Late Quaternary Evolution of Songkhla Coast, Southern Thailand, Revealed by OSL Dating. *Chiang Mai Journal of Science*, 46, 152-164.

Prescott, J. R., & Hutton, J. T. (1994). Cosmic ray contributions to dose rates for luminescence and ESR dating: Large depths and long-term time variations. *Radiation Measurements*, 23(2), 497-500. doi:10.1016/1350-4487(94)90086-8

Polwichai, S. (2017). *Paleo Sea-level Change of Laem Pho, Amphoe Chaiya, Changwat Surat Thani*. (Master's degree), Chulalongkorn University, Bangkok. Retrieved from http://cuir.car.chula.ac.th/handle/123456789/60056

Readhead, M. L. (1987). Thermoluminescence dose rate data and dating equations for the case of disequilibrium in the decay series. *International Journal of Radiation Applications and Instrumentation. Part D. Nuclear Tracks and Radiation Measurements*, *13*(4), 197-207. doi:10.1016/1359-0189(87)90037-9

Reimann, T., Naumann, M., Tsukamoto, S., & Frechen, M. (2010). Luminescence dating of coastal sediments from the Baltic Sea coastal barrier-spit Darss–Zingst, NE Germany. *Geomorphology*, *122*(3), 264-273. doi:10.1016/j.geomorph.2010.03.001

Sainakum, A., Jittangprasert, P., Sompongchaiyakul, P., & Jirapinyakul, A. (2021). Using n-alkanes as a proxy to reconstruct sea-level changes in Thale Noi, the west coast of the Gulf of Thailand. *Journal of Asian Earth Sciences*, *213*, 104740. doi:10.1016/j.jseaes.2021.104740

Singh, A. K., Pattanaik, J. K., Gagan, & Jaiswal, M. K. (2017). Late Quaternary evolution of Tista River terraces in Darjeeling-Sikkim-Tibet wedge: Implications to climate and tectonics. *Quaternary International, 443*, 132-142. doi:10.1016/j.quaint.2016.10.004

Sinsakul, S. (1992). Evidence of quaternary sea level changes in the coastal areas of Thailand: a review. *Journal of Southeast Asian Earth Sciences*, *7*(1), 23-37. doi:10.1016/0743-9547(92)90012-Z

Surakiatchai, P. (2006). *Classification of gastropoda and bivalvia fossils from the Khao Sam Roi Yod National Park, Prachuap Khiri Khan Province, Thailand* (Master's thesis, Chulalongkorn University, Bangkok, Thailand). Retrieved from http://www.thaithesis.org/detail.php?id=1082545000163

Surakiatchai, P., Choowong, M., Charusiri, P., Charoentitirat, T., Chawchai, S., Pailoplee, S., Bissen, R. (2018). paleogeographic reconstruction and history of the sea level change at Sam Roi Yot National Park, Gulf of Thailand. *Tropical Natural History*, *18*(2), 112-134.

Surakiatchai, P., Songsangworn, E., Pailoplee, S., Choowong, M., Phantuwongraj, S., Jirapinyakul, A., & Charusiri, P. (2019). Optically stimulated luminescence dating reveals rate of beach ridge and sand spit depositions from the upper Gulf of Thailand. *Songklanakarin Journal of Science and Technology*, *41*, 1136-1145.

Takashima, I., & Honda, S. (1989). Comparison between K-Ar and TL dating results of pyroclastic flow deposits in the Aizutajima area, Northeast Japan. *Journal of the Geological Society of Japan*, *95*, 807-816.

Törnqvist, T. E., Bick, S. J., González, J. L., van der Borg, K., & de Jong, A. F. M. (2004). Tracking the sea-level signature of the 8.2 ka cooling event: New constraints from the Mississippi Delta. *Geophysical Research Letters*, *31*(23). doi:10.1029/2004GL021429

Verstappen, H. T. (1980). Quaternary climatic changes and natural environment in SE Asia. *Geo Journal*, *4*(1), 45-54. doi:10.1007/BF00586754

Williams, H., Choowong, M., Phantuwongraj, S., Surakietchai, P., Thongkhao, T., Kongsen, S., & Simon, E. (2016). Geologic records of Holocene typhoon strikes on the Gulf of Thailand coast. *Marine Geology*, *372*, 66-78. doi:10.1016/j.margeo.2015.12.014

Wilford, J. (2012). A weathering intensity index for the Australian continent using airborne gamma-ray spectrometry and digital terrain analysis. *Geoderma*, *183-184*, 124-142. doi:10.1016/j.geoderma.2010.12.022